Rock Mechanics and Rock Engineering (2018) 51:3895–3906
https://doi.org/10.1007/s00603-018-1544-8

ORIGINAL PAPER

# Impact of Fluid Acidity on the Time-Dependent Initiation of Hydraulic Fractures in Carbonate Rocks

**Q. Lu[1] · G. Lu[1] · R. Prioul[3] · G. Aidagulov[4] · A. P. Bunger[1,2]**

Received: 13 February 2018 / Accepted: 30 June 2018 / Published online: 19 July 2018


**Abstract**
Carbonate-rich rocks are commonly encountered in oil and gas reservoirs, and as such, mechanisms of hydraulic fracture initiation and growth in carbonates are important for effective reservoir stimulation. Thus motivated, this paper shows the impact of acidic fluid on the hydraulic fracture initiation in laboratory experiments. The results demonstrate that compared to water injection, acid injection results in more rapid initiation of the hydraulic fractures under so-called static fatigue or pressure-delay conditions wherein a certain pressure, insufficient to instantaneously generate a hydraulic fracture, is maintained until a hydraulic fracture grows. Acid injection also is shown to generate a dissolution cavity in the vicinity of the wellbore, and the breakdown of the specimen is observed to be explosive in the case of acid injection, probably due to the generation and the subsequent rapid expansion of carbon dioxide as a part of the dissolution reaction. Finally, the time to breakdown is shown to be related not only to the magnitude of the wellbore pressure, but also to the apparent permeability of the specimen. Altogether, the results indicate first that acid injection has the potential to improve the initiation of multiple hydraulic fractures within multistage hydraulic fracturing of horizontal wells by decreasing the time required for initiation at subcritical wellbore pressures. The results also show that the current theoretical framework can capture the overall negative exponential relationship between the time to breakdown and the wellbore pressure, but it is insufficient to account for the secondary dependence on rock permeability.

**Keywords** Hydraulic fracturing · Carbonate rocks · Static fatigue · Subcritical crack growth · Horizontal wells

**List of symbols**

| | |
|---|---|
| $\sigma_{\theta\theta}^{\max}$ | Maximum tangential Biot effective stress |
| $\sigma_{\mathrm{T}}$ | Tensile strength of the rock |
| $\beta$ | Poroelastic parameter |
| $p_{\mathrm{w}}$ | Wellbore pressure |
| $\eta$ | Poroelastic constant |
| $\nu$ | Poisson's ratio |
| b | Biot coefficient |
| $\sigma_1$ | Larger in situ stresses transverse to wellbore |
| $\sigma_2$ | Lesser in situ stresses transverse to wellbore |
| $\tau$ | Life time of specimen |
| $U_0$ | Initial energy barrier |
| T | Absolute temperature |
| k | Boltzmann's constant |
| $\gamma$ | Microstructural parameter |
| $\tau_{\mathrm{o}}$ | Characteristic time independent of material |

✉ A. P. Bunger
BUNGER@pitt.edu

[1] Department of Civil and Environmental Engineering, University of Pittsburgh, Pittsburgh, PA, USA

[2] Department of Chemical and Petroleum Engineering, University of Pittsburgh, Pittsburgh, PA, USA

[3] Schlumberger-Doll Research, Cambridge, MA, USA

[4] Schlumberger Dhahran Carbonate Research, Dhahran, Kingdom of Saudi Arabia

## 1 Introduction

Subcritical crack growth has been observed and characterized for a wide range of rock types and perhaps most notably, has been classically considered to have a profound effect on the development of natural fracture sets (Olson 1993, 2004; Gale et al. 2007). However, this long-recognized characteristic of rock failure has only recently been considered as a mechanism impacting hydraulic fracturing (HF) initiation (Bunger and Lu 2015; Lu et al. 2015, 2017). The time-delayed initiation of hydraulic fractures resulting from interplay between fluid injection and subcritical crack growth is expected to play an important role in the effectiveness

of hydraulic fracturing in challenging formations where breakdown cannot be achieved with typical limits on pumping equipment. The mechanism of delayed initiation is also argued to be potentially critical for initiation of multiple hydraulic fractures within each stage of a horizontal well stimulation, wherein growth of other hydraulic fractures in each stage can lead to reduced pressure available to initiate fractures from all entry points (Lu et al. 2017). In contrast to the delayed initiation concept, over the past few decades, hydraulic fracture initiation has been classically considered to be governed by a binary criterion determining whether the wellbore pressure can induce large enough tensile stress, which meets or exceeds the tensile strength of the rock (Hubbert and Willis 1957; Haimson and Fairhurst 1967; Detournay and Carbonell 1997). Either the pressure is sufficient to generate a hydraulic fracture, or it is not.

Recent efforts have shown this binary criterion can sometimes provide an incomplete picture. Rather, the pressurization of a wellbore to a level insufficient for instantaneous initiation can instead lead to delayed initiation. Such behavior has been demonstrated experimentally in the laboratory for sandstone and granite (Lu et al. 2015; Uwaifo 2015).

At the same time, there are still some open questions. First, while the specimen lifetime, referring to the time between the start of the pressurization and the loss of specimen integrity due to hydraulic fracturing, has been shown to be dependent on wellbore pressure with an exponential, as would be consistent with static fatigue theory of materials (Zhurkov 1984), the scatter in the data indicates that the pressure is probably not the only critical characteristic of the initiation (Lu et al. 2015; Uwaifo 2015). Second, all experiments to date have been conducted under conditions where no chemical interaction/reaction is expected between the rock and fluid. Here we present laboratory research aimed at this second issue, addressing the question of how the pressure-delay initiation phenomenon occurs in an acidic environment in a carbonate rock. There are reasons to expect that acidic fluid will have an impact. Past experimental analyses (e.g., Hill et al. 2007; Wu and Sharma 2017) show that interaction with acid can weaken the rock matrix and make the rock easier to break. That idea inspires us to hypothesize that the acidic fluid injection will reduce the breakdown period and accelerate the speed of the delayed initiation. We evaluate experimentally, for the first time, the potential for hydrochloric acid to reduce the delayed initiation time for hydraulic fractures.

To achieve these goals, delayed hydraulic fracture initiation laboratory experiments are conducted on limestone samples by injecting both pure water and 15% hydrochloric acid (HCl) with constant pressure. Besides the pressure-delay failure phenomenon, it is also observed in a few tests that the pressure fluctuated along with a brief burst of fluid injection some time prior to complete specimen breakdown. This phenomenon is explored in detail using acoustic emission (AE) detection.

Such experiments are necessarily carried out in a controlled, idealized manner, enabling interpretation by isolating the mechanism of interest. The experiments do not attempt to address issues related to the complexities of the associated field application, i.e., abnormalities in the wellbore geometry, rock heterogeneity, and/or impact of cement, casing, and perforation. Hence we focus on a particular phenomenon in a controlled environment recognizing that a variety of phenomena interact to determine behavior obtained in field applications.

The paper begins with theoretical background on hydraulic fracture initiation and static fatigue of rocks, reviewing the premise of Bunger and Lu (2015). We then move to the details of the experimental procedure, with the program consisting of both water and acid injection cases. Next we present detailed observations of the similarities and differences between the two groups, including results of the AE tests. Taken together, this theoretical background, procedure, and observation lead to conclusions about the importance of fluid acidity in the time-dependent initiation of hydraulic fractures, as well as unexpected results related to other mechanisms not yet explicitly accounted for by theory and which provide motivation for further study.

## 2 Theoretical Background

The theoretical considerations begin with a classical description of the stresses around a wellbore. According to the theories which were put forward by Hubbert and Willis ("H–W", 1957), Haimson and Fairhurst ("H–F", 1967), and systemized by Detournay and Carbonell (1997), the criteria for the rock breakdown, which in these theories are taken as synonymous with hydraulic fracture initiation is:

$$\sigma_{\theta\theta}^{\max} = \sigma_{\mathrm{T}} \tag{1}$$

Here, $\sigma_{\mathrm{T}}$ is the tensile strength of the rock and $\sigma_{\theta\theta}^{\max}$ is the maximum tangential Biot effective stress given by:

$$\sigma_{\theta\theta}^{\max} = \beta p_{\mathrm{w}} - \hat{\sigma} \tag{2}$$

Here $\beta$ is a poroelastic parameter given by:

$$\beta = \begin{cases} 1 & \mathrm{H-W(fast)} \\ 2(1-\eta) & \mathrm{H-F(slow)} \end{cases}, \tag{3}$$

where $\eta$ is a poroelastic constant between 0 and 0.5 and related to the Poisson's ratio $\upsilon$ and Biot coefficient $b$ as

$$\eta = \frac{b(1-2\nu)}{2(1-\nu)} \tag{4}$$

Additionally $p_{\mathrm{w}}$ is the wellbore pressure, and $\hat{\sigma}$ is the near-wellbore effective in situ stress contribution (adopting here the notation of Bunger and Lu 2015) given by:

$$\hat{\sigma} = \begin{cases} -\sigma_1 + 3\sigma_2 - p_0 & \text{H} - \text{W(fast)} \\ -\sigma_1 + 3\sigma_2 - 2\eta p_0 & \text{H} - \text{F(slow)} \end{cases} \quad (5)$$

Here $\sigma_1$ and $\sigma_2$ are the greater and lesser of the pre-existing in situ stress components acting transverse to the wellbore, respectively, and $p_0$ is the virgin pore pressure in the formation. Note that this relationship reduces to a simple proportionality between the maximum tensile stress and the wellbore pressure $p_w$ in the absence of in situ (i.e., confining) stresses. Note that the notation "H–W (fast)" indicates the expression from Hubbert and Willis (1957), which is shown to correspond to the fast pressurization case where the fluid is not able to penetrate the near-wellbore region prior to breakdown (as discussed in detail by Detournay and Carbonell 1997). Similarly, the notation "H–F (slow)" indicates the expression from Haimson and Fairhurst (1967), which corresponds to the slow pressurization case wherein the fluid is able to penetrate the rock in the near-wellbore region prior to breakdown.

Substitution of Eq. (1) into (2) gives a classical relationship defining the so-called breakdown pressure, that is, the wellbore pressure at which a hydraulic fracture initiates due to the induced near-wellbore tensile stress attaining the tensile strength of the rock. However, recent studies (Lu et al. 2015; Uwaifo 2015) have shown that the initiation of hydraulic fractures can occur even if the wellbore pressure is not large enough for the tensile stress to match the tensile strength. Specifically, the fracture is observed to initiate after some period of time with a lower wellbore pressure than is implied by the breakdown criterion (Fig. 1). Thus, the classical theory may be insufficient to explain many situations where breakdown is achieved at lower than predicted wellbore pressure.

To enhance the theory in light of experimental evidence, we follow Bunger and Lu (2015) and turn to the phenomenon by which materials have been shown to fail after some period when they are exerted by loading that cannot induce instantaneous failure. This phenomenon is called "static fatigue", and it is classically defined in the form of a kinetic equation (Zhurkov 1984) relating the time to breakage $\tau_0$ and the applied stress $\sigma$

$$\tau = \tau_0 e^{\frac{U_0 - \gamma\sigma}{kT}} \quad (6)$$

Here the product of Boltzmann's constant $k$ and absolute temperature $T$ represent energy associated with atomic-scale thermal oscillations. The material property $U_0$ is interpreted as the magnitude of the initial energy barrier determining the probability of breakage of interatomic bonds responsible for the material strength; it is interpreted to be very close in magnitude to the binding energy of atoms in materials (Zhurkov 1984). According to Eq. (6), by applying the load on the sample, the energy barrier will decrease linearly with the tensile stress σ, with proportionality constant γ being interpreted as a microstructural parameter associated with the translation of an applied macroscopic loading to the energy associated with microscopic-scale bond breakage. Finally, the characteristic time $\tau_o$ was found by Zhurkov (1984) to be independent of the structure and chemical nature, with magnitude of $10^{-13}$ s. This is on the order of the period of atomic-scale thermal oscillations. It also represents the minimum time required to rock failure when $U_0 - \gamma\sigma = 0$, also known as instantaneous breakdown and shown by Zhurkov (1984) to correlate well with the upper limit on crack propagation velocity corresponding to the speed of sound in the material. Note, however, in our experimental configuration, it is quite challenging and unpractical to approach and measure a time period with $10^{-13}$ s magnitude. Therefore, we define 1 s as the instantaneous breakdown time, which is more reasonable and applicable to our cases of quasi-static crack growth (i.e., with a finite velocity, but negligible inertia in the equations of motion).

The role of static fatigue theory brings the dependence on time into consideration for hydraulic fracture breakdown. By substituting Eq. (2) into Eq. (6) we obtain

$$\tau = \tau_0 e^{\frac{U_0 - \gamma(\beta p_w - \hat{\sigma})}{kT}} \quad (7)$$

Hence, for both confined ($\hat{\sigma} \neq 0$) and unconfined case ($\hat{\sigma} = 0$), the theory predicts a negative exponential relationship between the time to breakdown (i.e., the "lifetime") and the wellbore pressure. Such a relationship has been confirmed for hydraulic fracture initiation in granite (Lu et al. 2015) and sandstone (Uwaifo 2015). Here we will first validate this predicted behavior for limestone and then explore the impact of the acidity of the fluid.

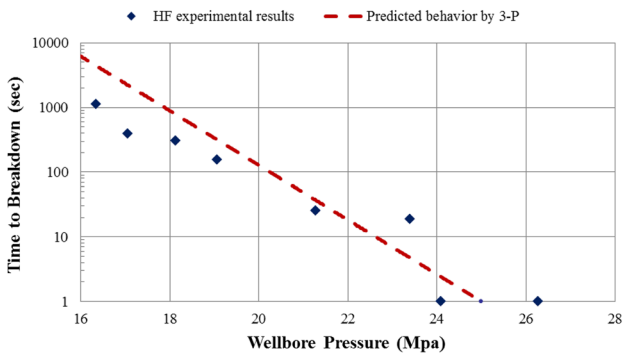


**Fig. 1** Hydraulic fracture experimental results on granite showing a negative exponential relation between wellbore pressure and time to hydraulic fracture breakdown (after Lu et al. 2015)

## 3 Experiments

### 3.1 Sample Preparation

Blocks of Kasota Valley Limestone were sourced and cut as 7.5 × 7.5 × 15 cm (3 × 3 × 6 in.) specimens. For consistency with the previous experiments in sandstone and granite (Uwaifo 2015; Lu et al. 2015), the injection hole was chosen to be 1.27 cm (0.5 in.) in diameter. It was drilled at the center point of the 7.5 × 7.5 cm face along the 15 cm side, through the entire thickness of the specimen, orthogonal to the bedding (i.e., akin to a vertically oriented wellbore), see Fig. 2. Next, a 21.6 cm (8.5 in.) long by 0.95 cm (3/8 in.) outer diameter stainless steel tubing with four perforation holes placed at symmetrical positions was put into the wellbore, working as the wellbore casing.

The completion of the analog wellbore is designed to generate an isolated, pressurized openhole section around the perforations. To do this, two rubber seal O-rings were placed between the wellbore surface and the tubing, with a 5 cm (2 in.) distance from each other as shown in Fig. 2. These work not only as centralizers, but also to isolate the pressurized region. Epoxy adhesive (in this case Sikadur 32) was then placed from both the top and the bottom of the specimen, allowing the adhesive to fill the open annulus space from the O-ring to the surface on both sides. This epoxy holds the tube in place and supports the O-rings holding high pressure. The epoxy adhesive is then allowed to dry at least 12 h so as to attain the maximum strength. Finally, a stainless steel fitting and a cap were fixed on one side of the tubing, while connecting the other side to the pumping system shown in Fig. 3. In general, the specimen would then be subjected to triaxial confining stress. However, in this work we wish to start with examining the influence of the wellbore pressure on delayed initiation of hydraulic fracture in the absence of the confining stress as it provides the most straightforward negative exponential relationship between wellbore pressure and time to failure (Eq. 7) with the least complicated experimental setup.

### 3.2 Experimental Apparatus

The sketch of the acid injection experimental apparatus is shown in Fig. 3. The main function of the equipment is to accomplish both the pumping of the fluid safely and effectively including the refilling during and after the experiments. The 260D ISCO high pressure syringe pump on the left side was used to generate the pressure. A shutoff valve was attached to the pump for safety reasons and it remained open throughout the experiment.

To prevent the corrosion of the tubing and the pump by the HCl, the stainless steel tubing was used only for parts of the system exposed to pure water, indicated in blue. It was replaced by the corrosion-resistant alloy material Monel for the acid handling part of the apparatus, which is marked in purple in Fig. 3. Then a mechanical separation was created so that the pump could inject non-corrosive fluid and the acidic fluid could be delivered to the specimen. To do this, a 150 cm long by 1.27 cm (0.5 in.) diameter Monel tubing, henceforth referred to as the interface container, was installed to serve as the acid container during the injection procedure. A PVC separation plug wrapped by an O-ring was placed in the tubing to separate the pump fluid and acid.

### 3.3 Experimental Procedure

Step 1: Acid Refill.

At the beginning of the experiment, the PVC plug should be at the specimen end of the interface container and all valves should be shut off. At this time, the interface container is filled with the (non-corrosive) pump fluid. The

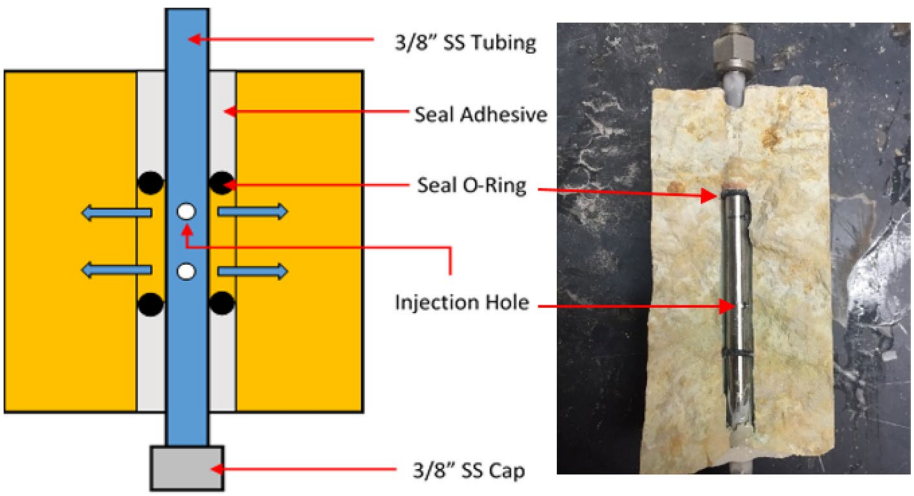


**Fig. 2** The cross section of the experiment sample

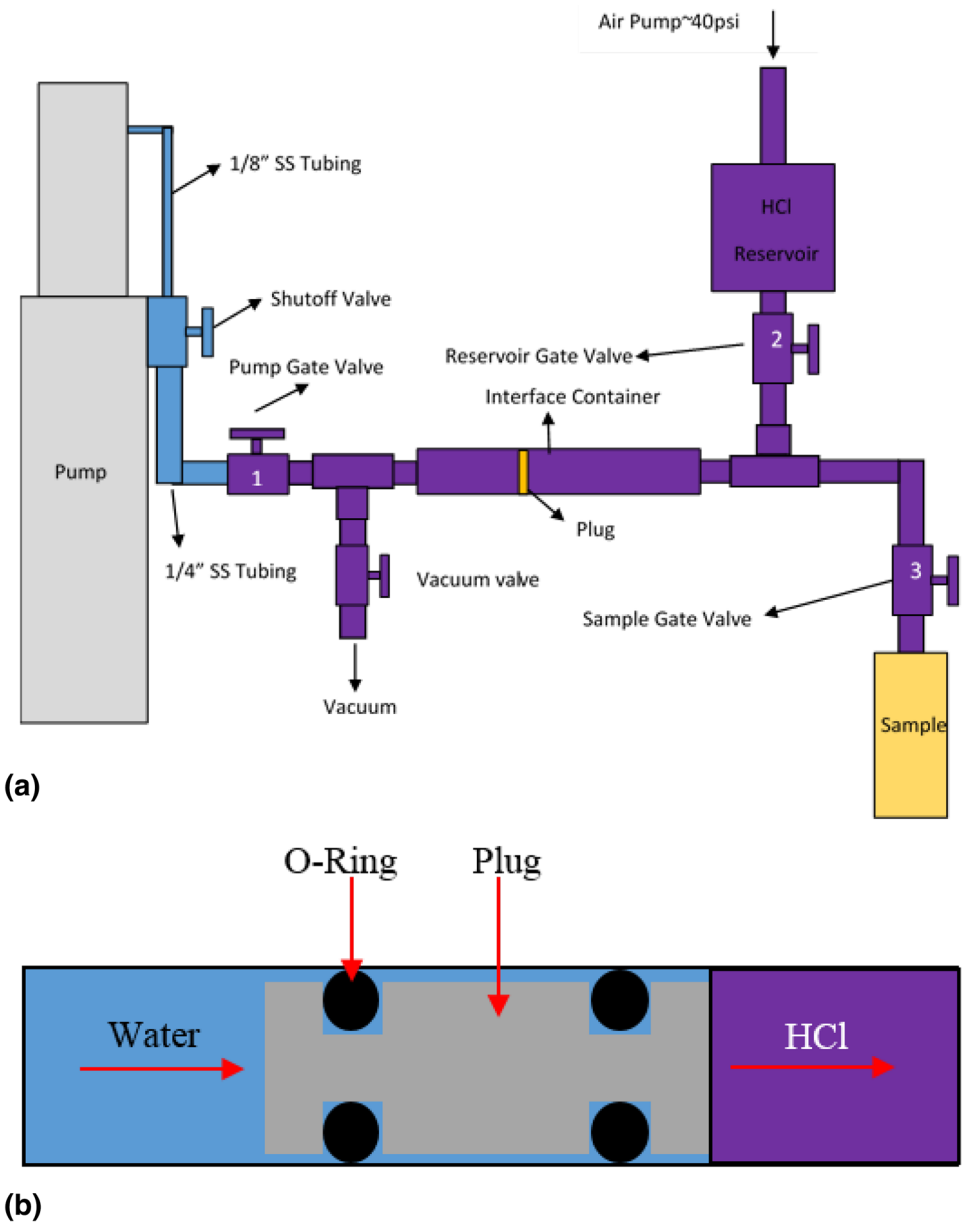


**Fig. 3** **a** The setup of the fluid injection system, and **b** detail of the PVC separation plug

acid refill entails forcing the acidic fluid (in our case, 15% HCl) into the interface container, driving the plug back to the pump end and in doing this, providing an interface container that is filled with the acidic fluid and ready for experimentation.

To begin the refilling, the acidic fluid was poured into the acid reservoir from the top opening. Then the PVC cap was screwed on the top to isolate the reservoir from air. The next step was to open the air pump valve, reservoir gate valve and vacuum valve consecutively. The air pressure, which is regulated down to 276 kPa (40 psi) to ensure it will not cause the low-pressure reservoir to rupture, pushes the acidic fluid back into the interface container until the plug hits the pump-side end. Finally, all valves are closed and prepared for the pressurization process.

Step 2: Pressurization.

Prior to commencing the pressurization, the first step was to activate the data acquisition system to record the injection pressure and the pump displacement (i.e., injected volume). Subsequently, the pump gate valve and the sample gate valve were turned on. Next, the system was pressurized to 345–689 kPa (50–100 psi) under constant pressure control to make sure that all tubing was fully filled with the acidic fluid and there is no leakage. Once the pressure reading on the pump was steady, a target pressure was applied and held constant until the hydraulic fracture was initiated. This target pressure was varied between the tests to explore the validity

of Eq. 7 for the prediction of the time dependence to breakdown $\tau$ on the wellbore pressure $p_w$. Note that initiation was typically visually apparent, and it also was evident due to a sudden increase in the pump displacement rate. After the initiation occurred, the pump was stopped as soon as possible, and all valves were turned off again.

### 3.4 Acoustic Emission Test Procedure

The internal damage to the rock due to hydraulic fracturing is accompanied by the generation of acoustic emission (AE) signals (after, e.g., Falls et al. 1992). AE detection system is utilized in two follow-up experiments on larger-size limestone blocks ($15 \times 15 \times 15$ cm) for measuring such localized energy release within the specimens.

In these two experiments, AE data were collected by the AE win 8 software on an Express-8 system from MISTRAS Group. The system uses 10, 1 cm diameter, 100 kHz to 1 MHz MISTRAS Group acoustic emission sensors placed on the blocks (Fig. 4). As shown in the figure, each surface (except for the bottom surface on which there was no AE sensor attached) contained two AE sensors. Using this monitoring system, both the location and the time of occurrence of the AE signals were recorded. Before conducting the delayed breakdown experiments, pencil lead break tests (after Hsu 1977) were carried out to make sure that all sensors are in contact and functioning properly. In addition, confining stresses ($\sigma_v$, $\sigma_H$, and $\sigma_h$ in Fig. 4) were applied by a custom-built ENERPAC true tri-axial loading machine. The load in each direction was evenly distributed along the entire surface of the specimen by placing flat loading plates between the loading actuator and the specimen. The applied confining stresses were: $\sigma_v = 6$ MPa; $\sigma_H = 6$ MPa; $\sigma_h = 4$ MPa, which is in contrast to the other experiments, which were unconfined.

## 4 Results

### 4.1 Water Group Data

There were in total 11 water experiments conducted to study the relationship between "lifetime" (time to breakdown) and the wellbore pressure for limestone in the absence of fluid acidity. As in the theory, $\tau$ is the lifetime and can be defined as the time from the moment the pressure reaches its target constant value to the moment the injection rate shoots up and the pressure drops, indicating macroscopic specimen failure, as shown in Fig. 5. In addition, the flow rate is recorded when it becomes steady, which is essentially the leakoff rate from the wellbore into the rock formation.

Table 1 presents the experimental data for the sample lifetime, wellbore pressure, and the flow rate. As we can see, the wellbore pressure varies from 2170 to 660 psi, corresponding to the lifetime extending from 1 to 580 s. Here, 2170 psi is found to correspond to the instantaneous breakdown pressure (about 1 s). A few tests run lower than 660 psi did not show any sign of specimen failure during for several thousand seconds, at which point the fluid reservoir was exhausted and the pressurization ceased. Thus, in our case, 660 psi is considered as the approximate lower limit for water pressure-delay initiation on the timeframe that is relevant to both lab experiments and for that matter, to hydraulic fracturing treatments in the field which are also often on the order of thousands of seconds in duration. Note also that it takes some time (around 10 s) for the pressure to stabilize at

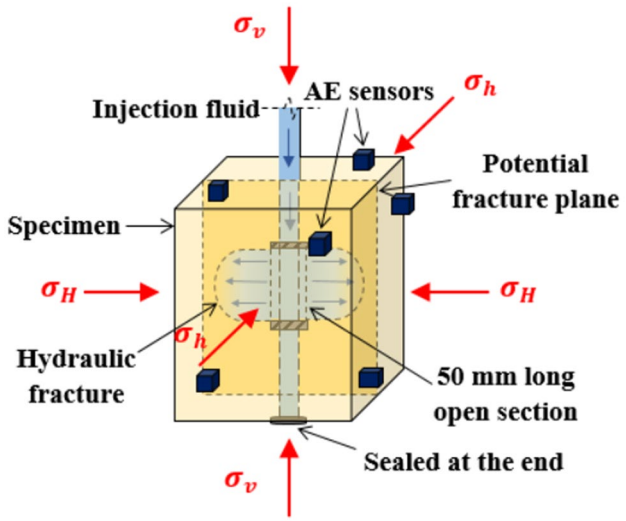


**Fig. 4** Sketch of specimen with AE sensor array

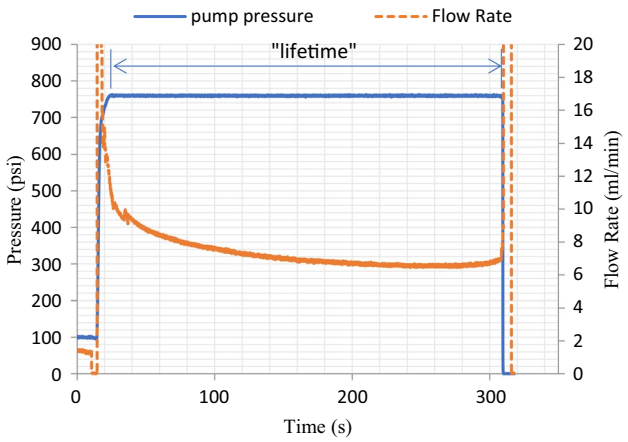


**Fig. 5** Example of water injection pressure and rate curves (test W20, target pressure is 760 psi), which shows the sample lifetime of about 280 s

**Table 1** Water experimental group data

| Test ID | Wellbore pressure (psi) | Lifetime $\tau$ (s) | Flow rate (ml/min) |
|---|---|---|---|
| W3 | 2170 | 1 | 185 |
| W4 | 1500 | 5 | 38 |
| W6 | 1340 | 21 | 16.5 |
| W19 | 1260 | 70 | 10.5 |
| W12 | 1150 | 20 | 30 |
| W15 | 1060 | 105 | 12.2 |
| W17 | 900 | 200 | 8 |
| W11 | 820 | 840 | 2.4 |
| W10 | 810 | 9 | 17.5 |
| W20 | 760 | 280 | 6.8 |
| W13 | 660 | 580 | 7.1 |

**Table 2** Acid experimental group data

| Test ID | Wellbore pressure (psi) | Lifetime $\tau$ (s) | Flow rate (ml/min) |
|---|---|---|---|
| A6 | 2040 | 1 | 23 |
| A3 | 1500 | 18 | 9.5 |
| A10 | 1350 | 8 | 43 |
| A8 | 1200 | 60 | 7 |
| A9 | 1100 | 22 | 18.5 |
| A2 | 1016 | 100 | 2.1 |
| A4 | 800 | 88 | 3.6 |
| A5 | 600 | 256 | 4.5 |
| A7 | 500 | 314 | 4 |
| A11 | 400 | 1380 | 1.1 |

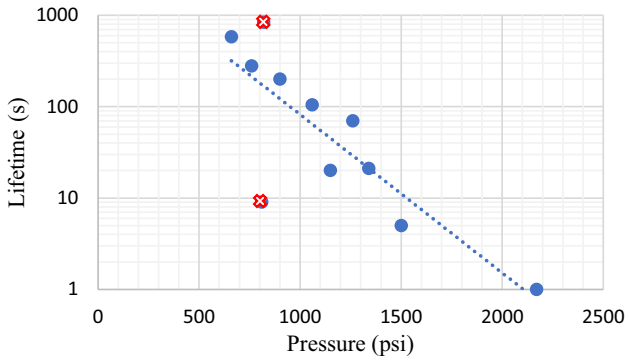


**Fig. 6** The data points show the relationship between the sample lifetime and target pressure for water experiments. Red points correspond to tests W10 and W11, which are taken as high and low permeability cases detailed in the discussion (Sect. 5.4)

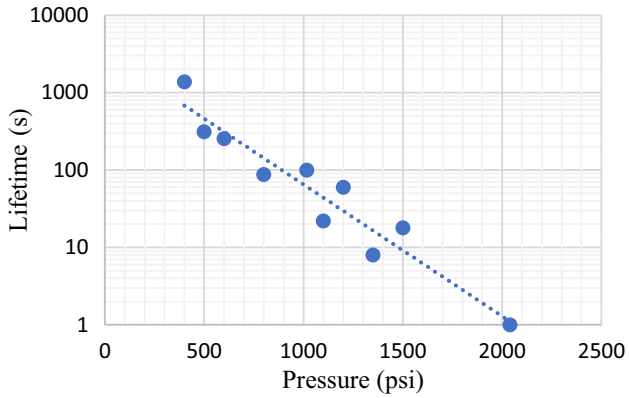


**Fig. 7** The data points show the relationship between the sample lifetime and target pressure for 15% HCl experiments

the set value, hence the lifetime is less precise for the higher pressure, shorter lifetime (i.e., less than 30 s) experiments.

From Fig. 6, we can see that the lifetime approximately follows the predicted negative exponential relationship with the wellbore pressure. This confirms that Zhurkov's (1984) theory as adapted for hydraulic fracturing by Bunger and Lu (2015) can provide a useful modeling framework for the pressure-delay phenomenon in this limestone in a similar manner to prior observations of time-delayed hydraulic fracture initiation in granite (Lu et al. 2015) and sandstone (Uwaifo 2015).

## 4.2 HCl Group Data

There were in total ten acid experiments conducted using 15% HCl, with the results shown in Table 2. As we can see from Fig. 7, in comparison with the water experimental group, the specimen lifetime in the acid group tests shows a tighter clustering around a negative exponential relationship with wellbore pressure.

Furthermore, the ability to attain failure at 400 psi wellbore pressure in the acid group tests indicates a reduction of the observed pressure lower limit required for the hydraulic fracture initiation within the practically relevant timeframe of a few thousand seconds. At the same time, the instantaneous breakdown pressure with the acid is almost the same as with the water. Altogether, it appears that the HCl does not make a substantial difference when the breakdown is rapid and hence the diffusion of the fluid into the rock and/or the dissolution of the rock do/does not have time to take place. In this rapid breakdown limit, the acidic fluid cases appear to generate breakdown at similar pressures and with similar delay time to pure water. However, at lower pressures, and hence larger times to breakdown, the fluid appears to be able to interact with the rock, which would explain the breakdown cases occurring at pressures that did not lead to breakdown with pure water.

## 5 Discussion

### 5.1 Explosive Behavior

Besides the differences in time to breakdown for the low pressurization cases, the fracture process observed in the acid experiments appears to be profoundly different from the water cases. The first striking observation is that the specimens exploded upon breakdown in the acid cases, probably due to the generation and the subsequent rapid expansion of carbon dioxide ($CO_2$) as a part of the dissolution reaction, namely, for limestone (e.g., Economides and Nolte 2000)

$$CaCO_3+2HCl \rightleftarrows CaCl_2+H_2O+CO_2 \quad (8)$$

The resulting blocks were fragmented for the acid cases (Fig. 8). In contrast, for the water cases, the breakdown and subsequent fracture growth led to just a small spurting of the fluid when the fracture reached the face of the specimen. The resulting blocks remained intact for the water cases (Fig. 8).

### 5.2 Dissolution Structures

The second main difference between the acid and the water cases is the development of a cavity in the region of the pressurized section of wellbore in the acid cases. The size of this cavity was up to several cubic centimeters, whereas in the water cases, there was no evidence of dissolution. There is observational evidence that it was created through wormhole formation (see, e.g., Fredd and Fogler 1998; Economides and Nolte 2000). This evidence includes pock-marked morphology and in some cases larger diameter (but still relatively short length) tunnels on the surface of the fractures. There was also a preponderance of fragmented material after the explosion, some of which could have been the intact skeleton between the wormholes (Fig. 9). Note that we do not observe systematic differences between dissolution or fragmentation-related morphologies for high-versus-low-pressure acid tests.

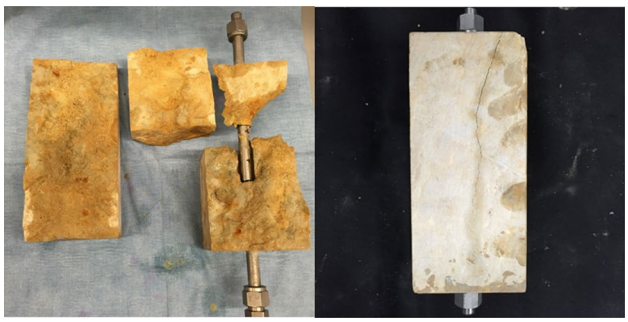

**Fig. 8** The 7.5×7.5×15 cm specimens after fracture initiation by HCl (left) and water (right)


**Fig. 9** Dissolution cavities created at 500 psi (left) and 1100 psi (right) target pressures

### 5.3 Impact of Acidic Fluid on Time to Initiation

Turning the attention back to the original question of whether the acid will reduce the time for initiation, further water versus acid comparison is made. Figure 10 shows the lifetime versus wellbore pressure for both experimental groups. Under the condition that both trend lines follow an exponential law, we can see that the acid experiment trend line is shifted down—a very little bit—underneath the water. However, the logarithmic scale understates the differences. Figure 11 shows the same data in linear scales, and here the impact of the acidic fluid is more clearly observed. Namely, for lifetimes in the range of 100–1000 s, the time to breakdown (lifetime) for the acidic fluid cases is 0.1–0.5 times the time to breakdown (lifetime) for comparable water cases. That is to say, at the same wellbore pressure, the acidic fluid treatment can reduce the time to breakdown by a factor of 2–10. Note that this reduction takes place over the practically relevant range because in field applications, the

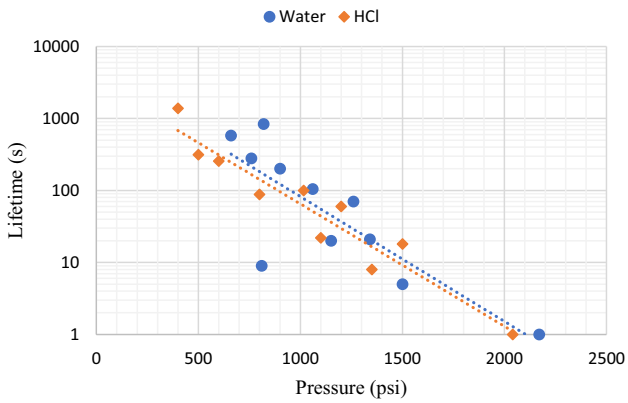


**Fig. 10** The pressure versus lifetime for both experimental groups shown in semi-log plot

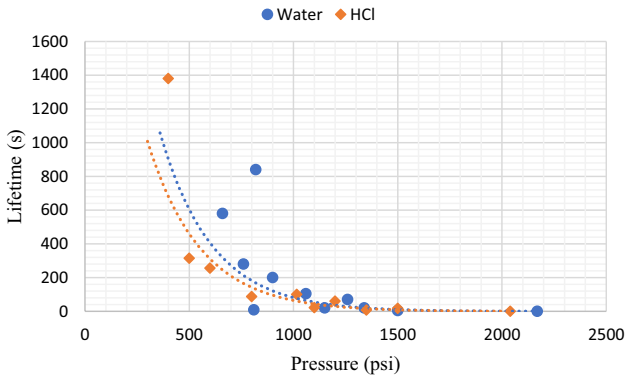


**Fig. 11** The pressure versus lifetime for both experimental groups shown in linear plot

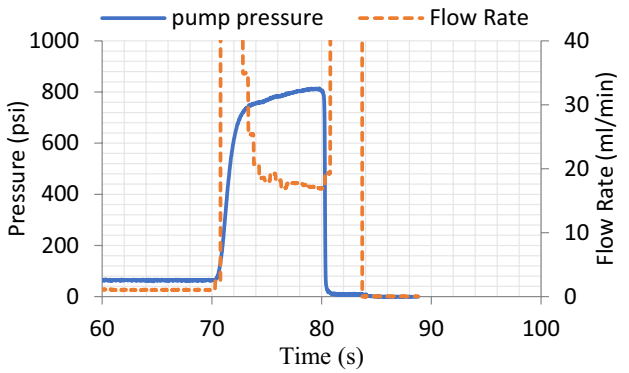


**Fig. 12** Pressure and flow rate versus time for the test W10, for which the sample broke after 9 s

treatments are thousands of seconds in duration. Thus, the delayed initiation in the order of hundreds of seconds would occur—for example, at entry points where hydraulic fractures did not initiate earlier in the pumping stage—still relatively early in a hydraulic fracturing treatment. Furthermore, time-delayed breakdown occurs within O ($10^3$) seconds for wellbore pressure around 30% of instantaneous breakdown pressure when water is used and at about 20% of the instantaneous breakdown pressure when acid is used. In contrast, initiation is observed within O($10^3$) seconds for wellbore pressure around 65% of instantaneous breakdown pressure for Coldspring Granite (Lu et al. 2015, see Fig. 1 in the current paper) and at around 45% of instantaneous breakdown pressure for Agra Red Sandstone (Uwaifo 2015). Therefore, it is apparent that Kasota Valley Limestone is prone to hydraulic fracture initiation at pressures further below the instantaneous breakdown pressure than the previously studied rock types.

## 5.4 Role of Permeability

Next we examine the possible origin for scatter in the data, beginning with water tests W10 and W11 (marked with red in Fig. 6), whose data points located far away from the trend of the other experiments. By contrasting the results for these two cases with each other (Figs. 12, 13), we can see there is a substantial variation of these specimens' lifetime, even though the wellbore pressure is pretty much the same. Then we should be aware that excluding the possible experimental and human error, there must have some additional phenomena, which led to the difference. The most intuitive variable is the flow rate, which should be proportional to the applied wellbore pressure via the hydraulic conductivity of the rock. We observe that the flow rate of test W10 is approximately double the flow rate of test W11 in spite of the two tests having the same wellbore pressure. Therefore, the implicit assumption of uniformity between samples is evidently not satisfied on these samples; the permeability of W10 must be much larger than W11.

Based on the phenomenon expounded above, we can put forward a hypothesis that besides the wellbore pressure, the lifetime of the specimen may also depend on the permeability or some other inherent rock properties associated with it. Specifically, the higher permeability specimens will lead to a shorter lifetime at the same pressure when compared to the lower permeability specimens. To test this hypothesis, the variation of the lifetime and the flowrate with respect to the pressure are shown in Fig. 14 for the water experiments and Fig. 15 for the acid experiments.

Careful inspection confirms the likely impact of the permeability. The dashed lines in the both figures correspond to best-fit (least-squares) trendlines, thus illustrating the approximate mean (average) value of lifetime and flow rate at different wellbore pressures. A clear tendency emerges, namely, when the permeability is lower than the mean value, evidenced by the flow rate plotting below the trendline, then the lifetime is observed to be larger than average, evidenced

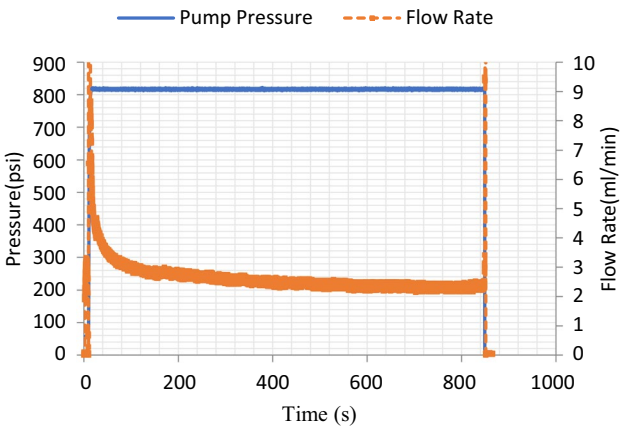


**Fig. 13** Pressure and flow rate versus lifetime for the test W11, which the sample broke after 840 s

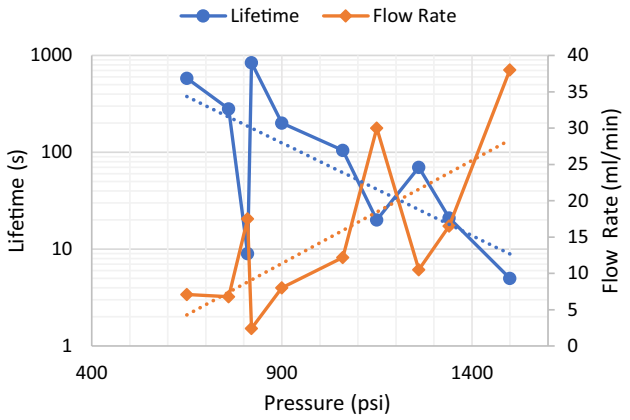


**Fig. 14** Lifetime and flow rate versus pressure for water experiments

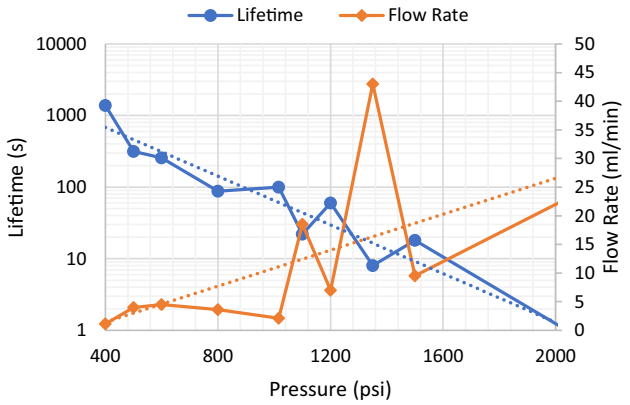


**Fig. 15** Lifetime and flow rate versus pressure for acid experiments

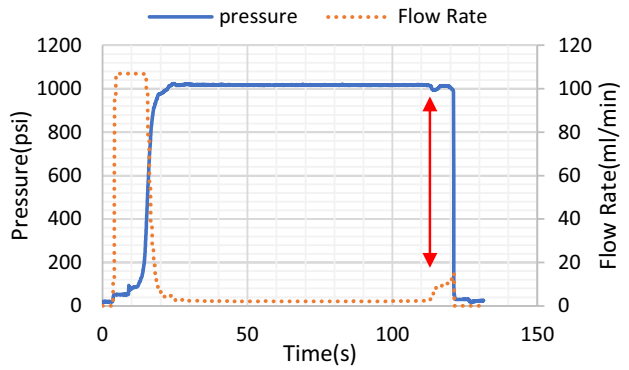


**Fig. 16** The injection pressure and flow rate curve for HCl group test A2

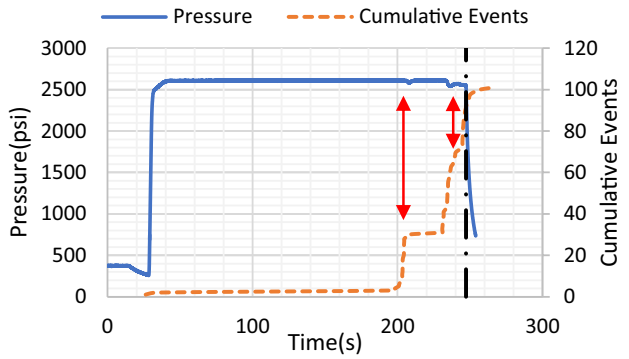


**Fig. 17** A water injection experiment with AE monitoring which had a pressure drop and increase of events before breaking down

by the lifetime plotting above the trendline. The converse is also true for higher than mean permeability cases—they lead to lower than average lifetime. It is striking to observe that this tendency is found to hold in all, but 2 of the 21 cases presented in the combined water and acid experiments. Thus, the impact of permeability, which is currently not considered in the theoretically based model, clearly must be accounted for as a part of future research.

## 5.5 Initiation Versus Breakdown

For most cases, the pressure is released when the specimen loses overall integrity, which means the fracture initiation and failure occur essentially simultaneously. However, a few exceptions are observed. The pressure and injection rate record for one of these cases, test A2 from the HCl group, is shown in Fig. 16. In this case, the wellbore pressure was held as constant by feedback loop control until a tiny drop-off took place at 110 s. This point corresponds to an increase in the injection rate, brought on by the pump's control loop in an effort to regain constant pressure. Such pressure drop accompanied by injection rate increase always occurs at the end of each experiment, at the point where the specimen loses integrity. However, here the pressure recovers for several seconds before macroscopic specimen failure. A similar behavior is shown in Fig. 17 for an experiment carried out by injection of water with AE detection. Here we observe two precursor pressure drops prior to the final loss of specimen integrity. Both of these pressure drops are accompanied by a burst of AE, indicative of fracture growth. Hence, these observations are consistent with an interpretation that fracture propagation event(s) preceded macroscopic specimen failure, where these precursor propagations were stable and based on the near cessation of AE, most likely arrested after their initial growth. Such arrested propagations have been observed in past experiments aimed at testing compounds for wellbore sealing (Guo et al. 2014), but in these prior experiments sealant material was mixed with the injected fluid so that the arrested initiations were reasonably interpreted as being "sealed". In the present experiments we see that while sealing is one possible mechanism for arresting initiating hydraulic fractures, such arrest can also occur without the use of sealant(s), presumably instead due to interaction of

the initiating fracture with the near-wellbore stress concentration. Interestingly, by examining crack growth equilibrium curves for fractures initiating from a wellbore, Detournay and Carbonell (1997) show that stable initiation can occur, depending on pressurization rate and ratio of intrinsic flaw length to wellbore radius, leading to the potential for arrest of an initiated fracture after it grows by an increment ranging up to one wellbore radius. Such an arrested initiation could be responsible for the observations portrayed in Figs. 16 and 17.

## 6 Conclusions

This paper describes an experimental research campaign motivated by the potential of the recently discovered time-dependent initiation phenomenon in hydraulic fracturing to be impacted by acidic environments. In total 21 experiments were performed: 11 with water and 10 with 15% HCl. Based on the analysis and the discussion illustrated above, we observe that time-delayed hydraulic fracture initiation occurs in limestone for both water and acid cases. In both groups of experiments, the lifetime of the specimen complies with the negative exponential relationship between time to failure ("lifetime") and wellbore pressure as predicted by Zhurkov's (1984) theory adapted for hydraulic fracture initiation by Bunger and Lu (2015).

In addition, we find that the hydrochloric acid can reduce the time needed for delayed initiation. With respect to reducing the initiation period, the performance of the acid treatment is more dramatic for the large lifetime (small pressure) cases, presumably since it is in these cases that the acid will have sufficient time in contact time with the rock matrix to induce dissolution and/or some other type of matrix weakening. Specifically, we find that acidic fluid treatment can reduce the time to breakdown by a factor of 2–10 relative to water treatments.

These observations confirm the hypothesized negative exponential relationship between time to breakdown and wellbore pressure and the hypothesized reduction of time to breakdown for acid cases. However, additional observations go beyond the original expectations and hypotheses. Notably, the hydraulic fracture initiation and subsequent growth in the acid experimental group were explosive, suggesting an unexpected importance of expanding gasses generated as a part of the dissolution reaction. Furthermore, a substantial dissolution cavity was observed to form near the wellbore inlet surface in the acid group cases.

The experimental observations also demonstrate that the wellbore pressure is not the only variable that impacts the specimen lifetime. The permeability, or the microstructural characteristics related to it, are also observed to systematically impact the result, with the specimens that are evidently the most permeable corresponding to smaller than expected time to initiation. This observation demonstrates that theories and accompanying laboratory experiments are necessarily put forward under idealized conditions that may not always be attained in reality. Nonetheless, the demonstration of basic phenomena under such controlled conditions can serve to guide the understanding and eventually development of models that better reflects the basic mechanisms that interact with one another to generate observed behaviors.

Finally, some experiments show evidence of fracture initiations that were apparently arrested rather than leading to macroscopic specimen failure. These arrested fracture initiations happen in both acid and water groups and without a clear mechanism for sealing. Hence, these most likely indicate that under constant wellbore pressure conditions, it is possible for fractures to arrest as they encounter varying stress conditions in the vicinity of the wellbore.

Taken together, these experiments demonstrate that time-dependent hydraulic fracture initiation occurs in limestone in a manner similar to other rocks, but with the important additional characteristic of being dependent upon fluid acidity. Furthermore, the effect is striking in the sense that hydraulic fractures are shown to initiate and grow at wellbore pressure far below what is required to induce instantaneous breakdown. Specifically, time-delayed breakdown occurs within $O(10^3)$ seconds for wellbore pressure around 30% of instantaneous breakdown pressure when water is used and at about 20% of the instantaneous breakdown pressure when acid is used. In this regard, the tendency for hydraulic fracture initiation within a practically relevant timeframe in limestone (or at least in Kasota Valley Limestone) is stronger than in previously tested species of granite and sandstone and as such, hydraulic fracture initiation models that ignore time dependence are particularly prone to error when making predictions for wells completed in limestone formations.

**Acknowledgements** This work was performed as a part of the MS dissertation research for QL at the University of Pittsburgh and with the support of Schlumberger. Some of this work was previously presented at the 51st US Rock Mechanics Symposium (Lu et al. 2017). This source of funding is gratefully acknowledged in addition to Schlumberger's permission to publish this paper. The design and fabrication contributions of Charles "Scooter" Hager (University of Pittsburgh) are also recognized. We also acknowledge contributions from other current and past University of Pittsburgh students including Garrett Swarm (now with Civil and Environmental Consultants, Inc.) and Ryan Winner (now at Texas A&M University).

## References

Bunger AP, Lu G (2015) Time-dependent initiation of multiple hydraulic fractures in a formation with varying stresses and strength. Soc Petrol Eng J 20(6):1317–1325

Detournay E, Carbonell R (1997) Fracture-mechanics analysis of the breakdown process in minifracture or leakoff test. SPE Prod Facil 12(03):195–199

Economides MJ, Nolte KG (2000) Reservoir stimulation, 3rd edn. Wiley, Chichester

Falls SD, Young RP, Carlson SR, Chow T (1992) Ultrasonic tomography and acoustic emission in hydraulically fractured Lac du Bonnet grey granite. J Geophys Res Solid Earth 97(B5):6867–6884

Fredd CN, Fogler HS (1998) Influence of transport and reaction on wormhole formation in porous media. AIChE J 44(9):1933–1949

Gale JFW, Reed RM, Holder J (2007) Natural fractures in the Barnett Shale and their importance for hydraulic fracture treatments. AAPG Bull 91(4):603–622

Guo Q, Cook J, Way P, Ji L, Friedheim JE (2014) A comprehensive experimental study on wellbore strengthening. In: IADC/SPE drilling conference and exhibition, 4–6 March, Fort Worth, Texas, USA, SPE/IACD 167957

Haimson B, Fairhurst C (1967) Initiation and extension of hydraulic fractures in rocks. Soc Petrol Eng J 7(03):310–318

Hill AD, Pournik M, Zou C, Malagon Nieto C, Melendez MG, Zhu D, Weng X (2007) Small-scale fracture conductivity created by modern acid fracture fluids. SPE Hydraulic Fracturing Technology Conference, College Station, Texas, 29–31 January, SPE 106272

Hsu N (1977) Acoustic emission simulator. U.S. Patent No. 4018084

Hubbert M, Willis D (1957) Mechanics of hydraulic fracturing. Trans AIME 210:153–168

Lu G, Uwaifo EC, Ames BC, Ufondu A, Bunger AP, Prioul R, Aidagulov G (2015) Experimental demonstration of delayed initiation of hydraulic fractures below breakdown pressure in granite. In: Proceedings 49th US rock mechanics/geomechanics symposium, San Francisco, CA, 28 June–1 July, ARMA 15–190

Lu G, Gordeliy E, Prioul R, Bunger AP (2017) Modeling initiation and propagation of a hydraulic fracture under subcritical conditions. Comput Methods Appl Mech Eng 318:61–91

Olson JE (1993) Joint pattern development: Effects of subcritical crack growth and mechanical crack interaction. J Geophys Res Solid Earth 98(B7):12251–12265

Olson JE (2004) Predicting fracture swarms—the influence of subcritical crack growth and the crack-tip process zone on joint spacing in rock. Geol Soc Lond Spec Publ 231(1):73–88

Uwaifo EC (2015) Time dependent initiation of multiple hydraulic facture in rock. MS Thesis, University of Pittsburgh

Wu W, Sharma MM (2017) Acid fracturing in shales: effect of dilute acid on properties and pore structure of shale. SPE Prod Oper 32(1):51–63

Zhurkov SN (1984) Kinetic concept of the strength of solids. Int J Fract 26(4):295–307